ISBN: 978-3-95450-248-6 ISSN: 2673-5490 doi: 10.18429/JACoW-IPAC25-TUPB013

TOWARDS AXION SEARCHES WITH POLARIZED HADRON BEAMS AT GSI/FAIR

D. Gu*[1,2,3], A. Lehrach[2,3], J. Pretz[2,3]
[1]GSI Helmholtzzentrum für Schwerionenforschung GmbH, Darmstadt, Germany
[2]Forschungszentrum Jülich, Jülich, Germany
[3]also at III. Physikalisches Institut B, RWTH Aachen University, Aachen, Germany
on behalf of the JEDI Collaboration

Abstract

Axions, originally introduced to solve the strong CP problem, are leading dark matter candidates appearing in various Standard Model extensions. At low masses, axion-like particle (ALP) dark matter behaves as a classical field, potentially detectable when its frequency resonates with a beam's spin-precession frequency. The JEDI collaboration's proof-of-principle experiment at COSY set upper limits on oscillating EDMs caused by ALPs, though no signals were observed. This paper discusses COSY results and recent efforts to explore the feasibility of conducting axion search experiments using existing accelerators at GSI/FAIR with polarized hadron beams.

INTRODUCTION

The strong CP problem in quantum chromodynamics predicts the existence of axions [1], which are leading dark matter candidates and arise naturally in many Standard Model extensions. These hypothetical particles, along with their generalized counterparts, axion-like particles (ALPs), interact with Standard Model fields via distinctive couplings. Of particular interest is the ALP–gluon coupling, which induces an oscillating Electric Dipole Moment (oEDM). For sub-μeV ALPs, the oEDM d takes the form [2, 3]:

$$d(t) = d_{\mathrm{DC}} + d_{\mathrm{AC}} \cos(\omega_a t + \varphi_0), \tag{1}$$

where $\omega_a = m_a c^2/\hbar$ defines the oscillation frequency directly related to the ALPs mass, φ_0 is an unknown phase. When the ω_a matches the spin precession frequency of polarized beams in storage rings, a vertical polarization builds up from an initially horizontal one. This resonance can be measured with a polarimeter via the left–right asymmetry.

Storage ring experiments offer two ALP search strategies: broad mass scans using energy variation and spin techniques, and focused measurements to verify specific mass signals with enhanced sensitivity [4]. The first proof-of-principle experiment in a storage ring was conducted by the JEDI collaboration at COSY using a 0.97 GeV/c polarized deuteron beam. Although no ALP signal was detected, the experiment demonstrated the viability of the storage ring approach and set upper limits on the oEDM in a narrow mass window near 5×10^{-9} eV [5].

Building on COSY's pioneering work and its closure, we recently proposed using the polarized beam source previously operated at COSY to realize polarized particle beams with a polarized target at the existing GSI/FAIR accelerator complex [6]. This offers opportunities to continue the search for ALPs in storage rings.

* daoning.gu@rwth-aachen.de

SPIN COHERENCE TIME (SCT)

The main challenge for storage ring based ALPs searches lies in maintaining polarization. In a storage ring, the spin tune $\nu_s = \gamma G$ (with G the gyromagnetic anomaly) governs spin precessions per revolution. As illustrated in Figure 1, for polarized beams the initial horizontal spin alignment depolarizes due to the beam momentum spread. This spread induces an energy-dependent spin tune spread through changes in γ, thus ultimately destroying polarization coherence.

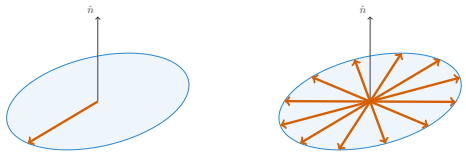

Figure 1: Illustration of spin coherence. Left: initial spin alignment. Right: decoherence due to spin tune spread.

The spin coherence time (SCT) is the time it takes for the polarization to decay to $1/e$ of its initial value. Since the statistical sensitivity of oEDM measurements scales inversely with SCT ($\sigma_{\mathrm{stat}} \propto 1/\tau_{\mathrm{SCT}}$), achieving a sufficiently long SCT (> 1000 s) becomes essential.

Theoretical Approach of SCT Optimization

Spin tune spread $\Delta\nu_s = \Delta\gamma G$ depends on particle energy. RF cavity bunching suppresses first-order effects, while second-order contributions from betatron motion and momentum deviations are quantified in [7, 8]:

$$\Delta\delta_{\mathrm{eq}} = \frac{\gamma_s^2}{\gamma_s^2\alpha_0 - 1}\left[\frac{\delta_m^2}{2}\left(\alpha_1 - \frac{\alpha_0}{\gamma_s^2} + \frac{1}{\gamma_s^4}\right) + \frac{\pi}{2L}(\varepsilon_x\xi_x + \varepsilon_y\xi_y)\right] \tag{2}$$

Here, α_0 and α_1 are the first- and second-order momentum compaction factors, γ_s the Lorentz factor of the synchronous particle, $\delta_m \equiv \Delta p/p$ the momentum deviation, $\xi_{x,y}$ the chromaticities, $\varepsilon_{x,y}$ the Courant–Snyder invariants, L the ring length, and $\Delta\delta_{\mathrm{eq}}$ the equilibrium energy shift.

ISBN: 978-3-95450-248-6 ISSN: 2673-5490 doi: 10.18429/JACoW-IPAC25-TUPB013

Under defind lattice conditions, the parameters α_1, ξ_x, and ξ_y dictate $\Delta\nu_s$, governing three decoherence mechanisms: momentum spread and horizontal/vertical betatron motion. This requires at least three sextupole families to be placed at large β_x, β_y, and D locations.

FEASIBILITY STUDY AT GSI/FAIR

The Experimental Storage Ring (ESR) at GSI can stores ions ranging from protons ($Z = 1$) to uranium ($Z = 92$), achieving energies up to 2208 MeV (protons) and 555 MeV/u (uranium) [9]. Electron cooling enables low emittance. Figure 2 shows the ESR optics with betatron tunes $Q_x = 2.36$, $Q_y = 2.28$.

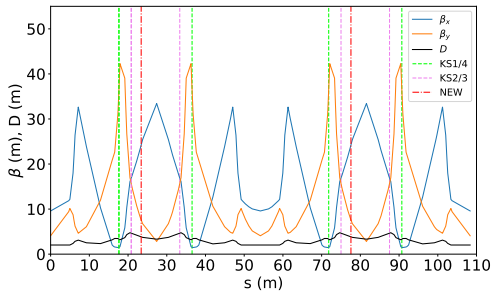

Figure 2: ESR optical functions showing β_x (blue), β_y (orange), and dispersion D (black). Vertical dashed lines indicate sextupole positions: existing families (green, purple) and proposed new locations (red) for three-family optimization.

Numerical Approach of SCT Optimization

We employ systematic sextupole optimization based on the functional dependence of SCT on magnet currents [10]:

$$\frac{1}{\tau} = |A + a_i I_i| \cdot (\Delta x)^2 + |B + b_j I_j| \cdot (\Delta y)^2 + |C + c_k I_k| \cdot \left(\frac{\Delta p}{p_0}\right)^2, \quad (3)$$

where τ denotes the SCT, Δx and Δy represent transverse particle deviations, and $\Delta p/p$ is the relative momentum deviation. The quadratic terms Δx^2 and Δy^2 correspond to horizontal and vertical emittance contributions respectively. The coefficients A, B, and C quantify decoherence rates without sextupole corrections, while I_i, I_j, I_k denote currents in distinct sextupole families with the corresponding coefficients a_i, b_j, c_k.

Numerical simulations using the Bmad software library [11] systematically vary both individual sextupole family strengths (k_2) and particle phase space parameters ($\Delta p/p$, Δx, Δy) in spin tracking simulations. Figure 3 presents simulation results for 1 GeV/c deuterons, showing the characteristic parabolic dependence of $\Delta\nu_s$ on the relative momentum deviation $\Delta p/p$ and transverse displacements Δx, Δy.

The existing two-sextupole configuration (upper panel of Figure 3) fails to control vertical displacement dependence due to large β_x overlap with long sector dipoles. The lower panel shows the successful optimization after introducing a third sextupole family placed close to the dipoles, suppressing quadratic dependence and reducing $\Delta\nu_s$ variations to $\mathcal{O}(10^{-10})$, indicating significant SCT improvements.

Spin Resonances

Since the oscillation frequency of ALPs is unknown, a full energy range scan of the ESR is needed. In an ideal lattice, intrinsic spin resonances arise solely from vertical betatron oscillations [12], occurring when:

$$\gamma G = nP \pm Q_y, \quad (4)$$

where $P = 2$ corresponds to the twofold periodicity of ESR, n is an integer, and Q_y denotes the vertical betatron tune.

Figure 4 compares the simulated spin tune spread across the full energy range for deuteron and proton beams. For deuteron beams, $\Delta\nu_s$ shows gradual energy dependence while remaining distant from resonance regions. In contrast, proton beams encounter two prominent intrinsic resonances at Q_y and $6 - Q_y$, requiring careful working point selection to avoid these resonance regions.

Sextupole Positions

We investigated the position dependence of SCT optimization by placing additional sextupoles at various locations and performing long-term spin tracking with ensembles of 100 particles over 20 million turns. The results reveal fundamental differences between deuteron and proton beam optimization requirements.

For deuteron beams (upper panel of Figure 5), the optimized three key parameters (ξ_x, ξ_y, α_1) remain consistent across different installation positions. All simulated configurations preserve over 95% of the initial polarization throughout the tracking period, demonstrating robust optimization performance.

Proton beams present greater challenges, with $G_p \approx 12.5 G_d$, increasing the optimized $\Delta\nu_s$ from $\mathcal{O}(10^{-10})$ (for deuterons) to $\mathcal{O}(10^{-8})$ (for protons), and requiring sextupole strengths at least an order of magnitude higher. Figure 5 (lower) reveals critical instabilities: while short-term tracking suggests stable polarization at multiple locations, after 10^7 turns ($\sim$ 7 s), the total polarization begins to drop rapidly at several sextupole locations, with some falling below the SCT threshold. This behavior suggests that strong sextupole fields introduce nonlinear effects that limit long-term polarization stability.

These simulations emphasise the importance of long-term tracking for optimization assessment, and indicate that proton beam optimization will require more sophisticated approaches, potentially including new optimization methods or alternative lattice configurations.

ISBN: 978-3-95450-248-6 ISSN: 2673-5490 doi: 10.18429/JACoW-IPAC25-TUPB013

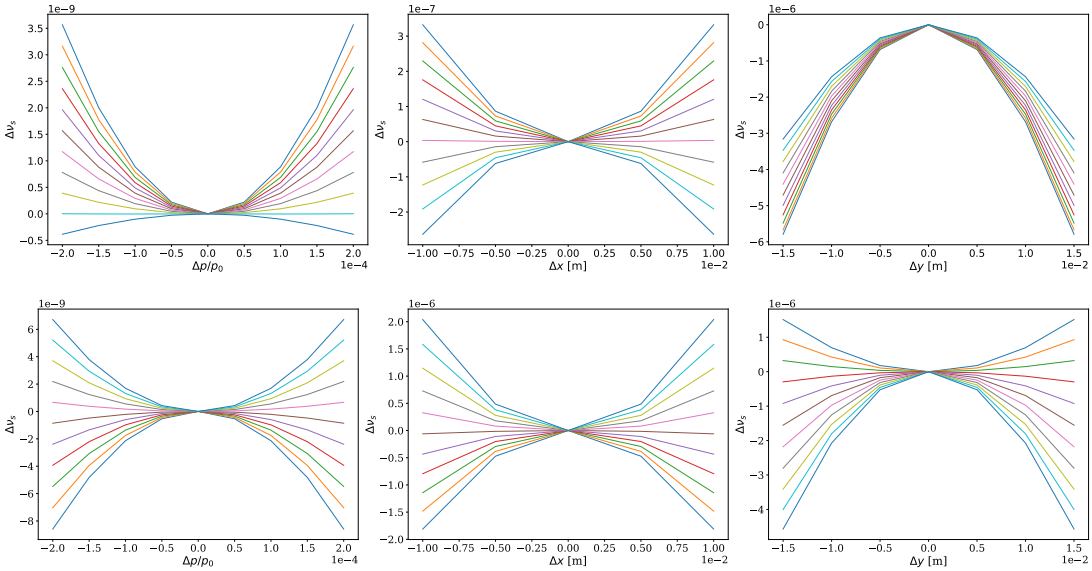

Figure 3: Simulated spin tune spread ($\Delta\nu_s$) vs. phase space variables for 1 GeV/c deuterons in ESR. Colors indicate normalized sextupole strengths k_2. Upper: existing two-sextupole configuration shows unoptimized parabolic dependencies (left-right: $\Delta p/p_0$, Δx, Δy), with Δy profiles clustered below $\Delta\nu_s = 0$. Lower: optimized three-sextupole configuration enables $\Delta\nu_s$ sign reversal through strategic sextupole placement near dipoles, achieving required zero-crossing for all variables.

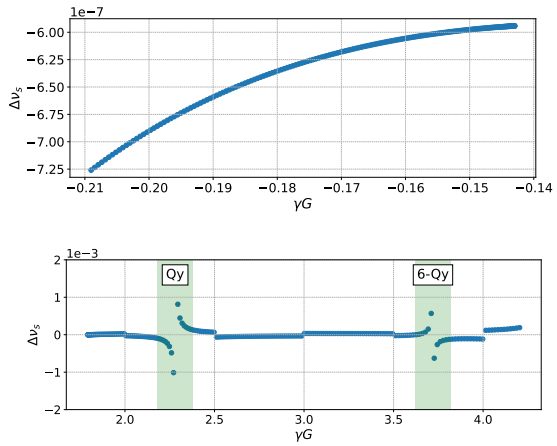

Figure 4: Energy dependence of spin tune spread in ESR. Upper: deuteron beam showing smooth variation without resonance interference. Lower: proton beam with two strong intrinsic resonance effects at Q_y and $6 - Q_y$ (highlighted in green).

CONCLUSION

Our simulations confirm that with an optimized three-sextupole configuration, deuteron beams achieve long spin coherence times across the ESR's operational energy range. Proton beams require at least an order of magnitude stronger sextupole fields due to their larger gyromagnetic anomaly, with careful working point selection required to avoid intrinsic spin resonances. Position-dependent optimization demonstrates that, while deuteron beams maintain polarization preservation, proton beams face greater challenges from sextupole-induced nonlinear effects. Future work will focus on developing improved optimization strategies for polarized proton beams in ALP searches at GSI/FAIR storage rings.

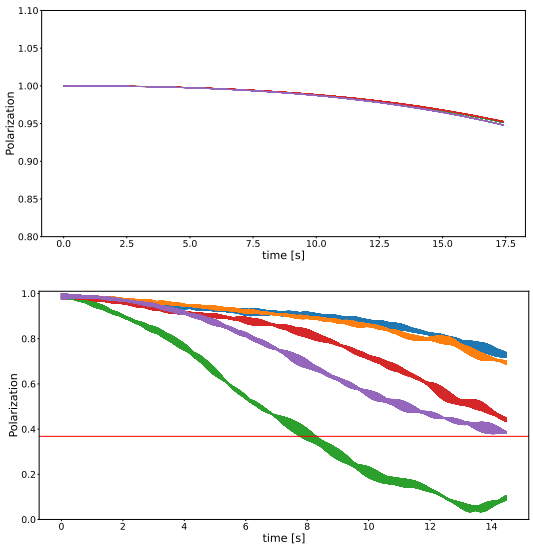

Figure 5: Long-term polarization evolution for 1 GeV/c beams with optimized sextupole settings in ESR. Different colors represent sextupole positions in both panels. Upper: deuteron beam showing nearly overlapping curves. Lower: proton beam demonstrating position-dependent polarization decay; red line marks the $1/e$ threshold τ_{SCT}.

ACKNOWLEDGEMENTS

The authors thank members of the JEDI Collaboration and of the Institut für Kernphysik of Forschungszentrum Jülich. Especially M. Vitz and A. Melnikov.

ISBN: 978-3-95450-248-6 ISSN: 2673-5490 doi: 10.18429/JACoW-IPAC25-TUPB013

REFERENCES

[1] R. D. Peccei and H. R. Quinn, "CP Conservation in the Presence of Pseudoparticles," *Phys. Rev. Lett.*, vol. 38, no. 25, pp. 1440–1443, Jun. 1977. doi:10.1103/PhysRevLett.38.1440

[2] P. W. Graham and S. Rajendran, "Axion Dark Matter Detection with Cold Molecules," *Phys. Rev. D*, vol. 84, no. 5, p. 055013, Sep. 2011. doi:10.1103/PhysRevD.84.055013

[3] P. W. Graham and S. Rajendran, "New Observables for Direct Detection of Axion Dark Matter," *Phys. Rev. D*, vol. 88, no. 3, p. 035023, Aug. 2013. doi:10.1103/PhysRevD.88.035023

[4] J. Pretz *et al.*, "Statistical Sensitivity Estimates for Oscillating Electric Dipole Moment Measurements in Storage Rings," *Eur. Phys. J. C*, vol. 80, no. 2, p. 107, Feb. 2020. doi:10.1140/epjc/s10052-020-7664-9

[5] S. Karanth *et al.*, "First Search for Axion-Like Particles in a Storage Ring Using a Polarized Deuteron Beam," *Phys. Rev. X*, vol. 13, no. 3, p. 031004, Jul. 2023. doi:10.1103/PhysRevX.13.031004

[6] T. Stöhlker *et al.*, "Towards Experiments with Polarized Beams and Targets at the GSI/FAIR Storage Rings," in *Proc. 19th Workshop on Polarized Sources, Targets and Polarimetry (PSTP'22)*, Mainz, Germany, Sep. 2022, paper 028, pp. 1–6. doi:10.22323/1.433.0028

[7] Y. Senichev, R. Maier, D. Zyuzin, and N. V. Kulabukhova, "Spin Tune Decoherence Effects in Electro- and Magnetostatic Structures", in *Proc. IPAC'13*, Shanghai, China, May 2013, paper WEPEA036, pp. 2579–2581.

[8] M. Rosenthal, "Experimental Benchmarking of Spin Tracking Algorithms for Electric Dipole Moment Searches at the Cooler Synchrotron COSY," Ph.D. thesis, RWTH Aachen University, Aachen, Germany, 2016.

[9] M. Steck and Y. A. Litvinov, "Heavy-Ion Storage Rings and Their Use in Precision Experiments with Highly Charged Ions," *Prog. Part. Nucl. Phys.*, vol. 115, p. 103811, Nov. 2020. doi:10.1016/j.ppnp.2020.103811

[10] G. Guidoboni *et al.*, "How to Reach a Thousand-Second in-Plane Polarization Lifetime with 0.97-GeV/c Deuterons in a Storage Ring," *Phys.Rev.Lett.*, vol. 117, no. 5, p. 054801, Jul. 2016. doi:10.1103/PhysRevLett.117.054801

[11] D. C. Sagan, "Bmad: A relativistic charged particle simulation library," *Nucl. Instrum. Methods Phys. Res. A*, vol. 558, pp. 356–359, 2006. doi:10.1016/j.nima.2005.11.001

[12] S. Y. Lee, *Spin Dynamics and Snakes in Synchrotrons*, World Scientific Publishing Co., Singapore, 1997. doi:10.1142/3233.